

## Chapter 4

### THE VIEW FROM SPACE

FAROUK EL-BAZ

National Air and Space Museum  
Smithsonian Institution  
Washington, D.C. 20560

#### ABSTRACT

*No systematic aerial photographs were ever obtained of the southwestern part of the Western Desert of Egypt. This lack of aerial photographs increases the value of images taken from space in studying the landscapes of this part of the desert. Coverage from space of the Western Desert of Egypt includes data from the manned missions of Gemini IV through XII, Apollo 7 and 9, Skylab 2, 3, and 4, and particularly the Apollo-Soyuz Test Project. It also includes images obtained by the unmanned Landsat spacecraft and weather satellites such as Meteosat. Detailed study of the landforms in this desert is hampered by the low resolution of space images and photographs. It is recommended that high resolution photographs of this desert be taken by the Large Format Camera on the Space Shuttle. Such photographs should be used in making large-scale topographic maps of the Western Desert, particularly its southwestern part. Other data that may be helpful in the future include the television (RBV) images from Landsat 3 and stereo, high resolution images from the French SPOT spacecraft.*

#### INTRODUCTION

The Western Desert occupies 681,000 km<sup>2</sup>, more than two-thirds the land area of Egypt. It is basically a rocky platform crossed in places by parallel belts of sand dunes. The generally flat terrain is broken by numerous depressions that enclose oases, and in the southwestern part, by the Gilf Kebir sandstone plateau and the granitic mountains of the Uweinat region (Said, 1962).

Aerial photographic coverage of this desert is patchy. The only part that is adequately photographed is the coastal strip; much of the coverage was obtained during World War II. Also, the western borders of the Nile Valley were photographed along with the oases, because of their value to agricultural and other economic development. The rest of the desert, particularly the southwestern part has never been systematically photographed by aerial cameras.

The lack of aerial photographs increases the value of those taken from Earth orbit. Since the advent of NASA's manned space program, orbital photographs have been used to provide information on remote, inaccessible and unexplored areas. Because of their large regional

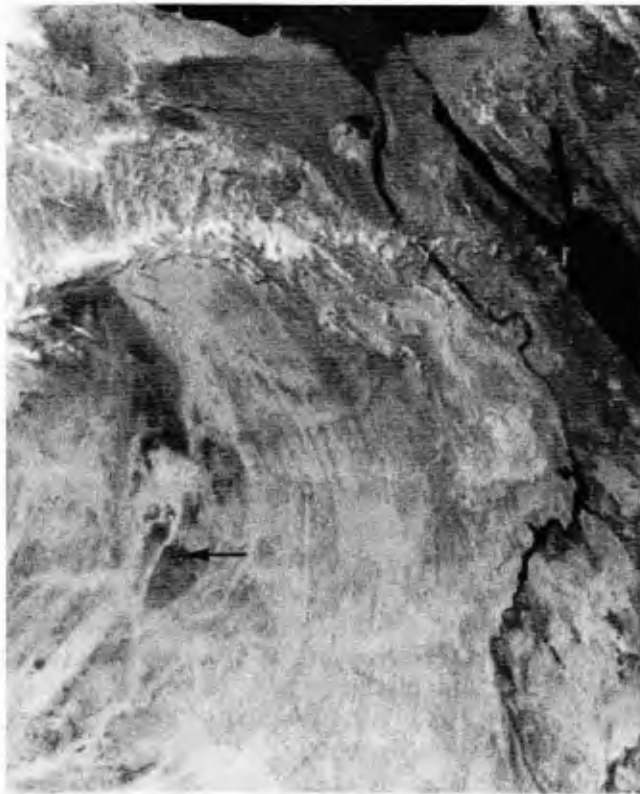


Figure 4.1      Enlargement of Meteosat image, at 2.5 km resolution, showing Egypt and parts of Libya and Sudan. Arrow points to the Uweinat Mountain (photo courtesy of G. Hunt).

coverage, these photographs provided a new perspective and an effective tool to study large-scale landforms. These photographs were later supplemented by images obtained by unmanned satellites such as Landsat and Meteosat (Fig. 4.1).

Table 4.1 lists the usable photographs and images covering parts of the deserts of Egypt. This list is here provided to allow ordering individual frames from NASA. The list includes those obtained on the Gemini IV through XII (55 frames), Apollo missions 7 and 9 (15 frames), Skylab missions 2, 3 and 4 (40 frames), Apollo-Soyuz Test Project (53 frames). Of nearly 500 images with less than 30% cloud cover from Landsat satellites, 65 reasonably cloud free images from Landsat 1 alone provide complete coverage of the deserts of Egypt (Table 4.2; Fig. 4.2).

#### ASTRONAUT PHOTOGRAPHS

All the American astronauts who orbited the Earth agreed that the view from space was wondrous. During the Mercury, Gemini and early Apollo flights it was quickly realized that trained astronauts were able to expertly describe observed phenomena and adequately photograph significant features (El-Baz, 1977).

Table 4.1 Earth Orbital Photographs Covering the Egyptian Deserts

<u>GEMINI IV</u>	<u>GEMINI XII</u>	<u>SKYLAB 2</u>	<u>APOLLO-SOYUZ</u>	
S-65-34664	S-66-62986	SL2-106-1142	70 mm Camera	70 mm Mapper
S-65-34665	S-66-62987	SL2-106-1143		
S-65-34668	S-66-63081	SL2-106-1144	AST-1-048	AST-16-1246
S-65-34776	S-66-63476		AST-1-049	AST-16-1247
S-65-34779	S-66-63477	<u>SKYLAB 3</u>	AST-1-050	AST-16-1248
S-65-34780	S-66-63478	SL3-115-1884	AST-1-051	AST-16-1249
S-65-34781	S-66-63479	SL3-115-1885	AST-2-126	AST-16-1250
S-65-34782	S-66-63480	SL3-115-1886	AST-2-127	AST-16-1251
S-65-34783	S-66-63481	SL3-115-1900	AST-2-128	AST-16-1252
S-65-34784	S-66-63482	SL3-115-1901	AST-2-129	AST-16-1253
	S-66-63529	SL3-115-1917	AST-2-130	AST-16-1254
<u>GEMINI V</u>	S-66-63530	SL3-115-1918	AST-2-131	AST-16-1255
S-65-45569	S-66-63531	SL3-115-1919	AST-2-132	AST-16-1256
S-65-45606	S-66-63532	SL3-115-1920	AST-2-133	AST-16-1257
S-65-45697	S-66-63533	SL3-115-1921	AST-2-134	AST-16-1258
S-65-45608	S-66-63534	SL3-118-2158	AST-2-135	AST-16-1259
S-65-45626		SL3-122-2620	AST-2-136	AST-16-1260
S-65-45736	<u>APOLLO 7</u>	SL3-129-3076	AST-2-137	
S-65-45778	AS7-5-1622	SL3-129-3077	AST-2-138	35 mm Camera
	AS7-6-1693		AST-2-139	
<u>GEMINI VII</u>	AS7-6-1694	<u>SKYLAB 4</u>	AST-2-140	AST-31-2633
S-66-63535	AS7-8-1905	SL4-138-3769	AST-9-553	AST-31-2634
S-65-63748	AS7-8-1906	SL4-138-3770	AST-9-554	AST-31-2635
S-65-63749	AS7-11-1999	SL4-138-3771	AST-9-555	
S-65-63849	AS7-11-2000	SL4-138-3772	AST-9-556	
S-65-63850	AS7-11-2003	SL4-138-3773	AST-9-557	
S-65-64006	AS7-11-2006	SL4-138-3790	AST-9-558	
	AS7-11-2008	SL4-138-3815	AST-13-843	
	AS7-11-2009	SL4-138-3869	AST-13-844	
<u>GEMINI X</u>		SL4-190-6993	AST-13-845	
S-66-45678		SL4-194-7219	AST-13-846	
S-66-45679	<u>APOLLO 9</u>	SL4-194-7220	AST-13-847	
S-66-45680	AS9-20-3176	SL4-194-7221	AST-13-848	
S-66-45681	AS9-20-3177	SL4-194-7222	AST-13-849	
	AS9-23-3521	SL4-194-7254	AST-13-850	
<u>GEMINI XI</u>	AS9-23-3522	SL4-194-7255	AST-13-851	
S-66-54528		SL4-194-7256	AST-13-852	
S-66-54529		SL4-194-7257		
S-66-54530		SL4-194-7258		
S-66-54531		SL4-194-7259		
S-66-54662		SL4-194-7261		
S-66-54663		SL4-194-7262		
S-66-54664		SL4-208-8143		
S-66-54776				
S-66-54777				
S-66-54778				
S-66-54893				
S-66-54895				

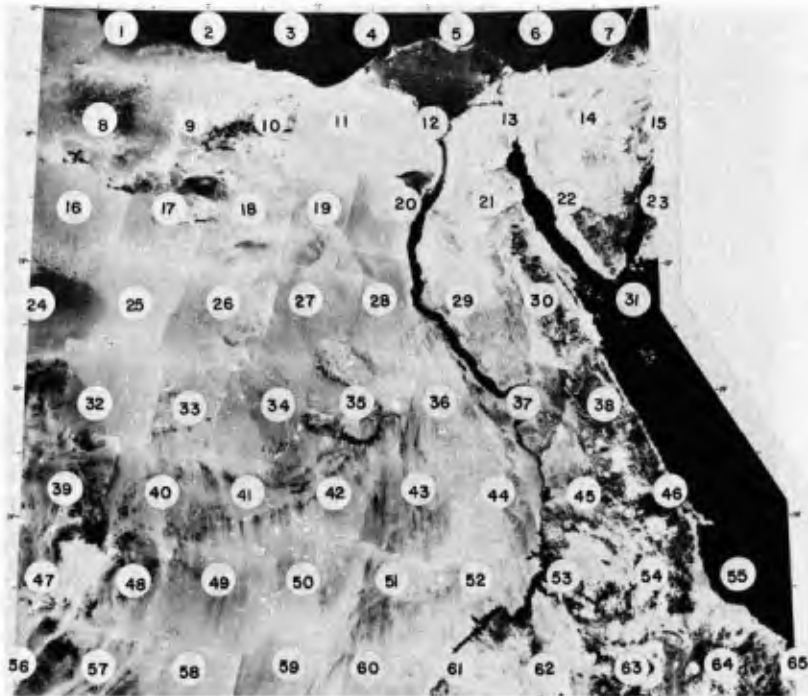


Figure 4.2 Landsat 1 coverage of Egypt; image numbers correspond to those listed in Table 4.2.

At the start of the American manned space flights, Mercury 6 through 9, an informal surface observation and photography experiment was conducted. The most valuable photographs were obtained on Mercury 9 by astronaut Gordon Cooper, who also made several observations that

Table 4.2 Landsat 1 Frames Providing Complete Coverage of Egypt.

1. E-1187-08230	17. E-1204-08182	33. E-1113-08132	49. E-1112-08083
2. E-1204-08173	18. E-1113-08123	34. E-1058-08065	50. E-1165-08023
3. E-1113-08114	19. E-1058-08060	35. E-1165-08014	51. E-1110-07570
4. E-1058-08051	20. E-1039-08001	36. E-1110-07561	52. E-1109-07511
5. E-1039-07592	21. E-1110-07552	37. E-1109-07502	53. E-1144-07453
6. E-1164-07541	22. E-1145-07493	38. E-1144-07444	54. E-1107-07394
7. E-1145-07484	23. E-1108-07434	39. E-1204-08194	55. E-1214-07341
8. E-1169-08231	24. E-1205-08243	40. E-1113-08135	56. E-1042-08193
9. E-1204-08180	25. E-1204-08185	41. E-1112-08080	57. E-1131-08144
10. E-1113-08121	26. E-1113-08130	42. E-1201-08022	58. E-1112-08085
11. E-1058-08053	27. E-1058-08062	43. E-1110-07563	59. E-1165-08025
12. E-1039-07595	28. E-1039-08004	44. E-1109-07504	60. E-1110-07572
13. E-1074-07541	29. E-1110-07554	45. E-1108-07450	61. E-1141-07285
14. E-1145-07491	30. E-1145-07500	46. E-1107-07392	62. E-1144-07455
15. E-1144-07432	31. E-1108-07441	47. E-1204-08200	63. E-1143-07401
16. E-1205-08241	32. E-1042-08182	48. E-1131-08141	64. E-1214-07344
			65. E-1091-07482

showed that he was able to see more than expected. These results generated considerable interest among the scientific community and encouraged plans for additional experiments on later missions.

Photographs on these missions were obtained using handheld Hasselblad cameras (Cortright, 1968). The 70 mm format allowed enlargement of the originals without affecting the sharpness of the photographs. Color film was used, which increased the value of the data. Scientists working with astronaut-obtained photographs were able to discriminate subtle changes recorded on the film because of the high sensitivity of the human eye to color. Particularly in photographs of desert regions, color was a significant factor, and variations in the color were found to be meaningful (El-Baz, 1978a), thus adding to the scientific content of space-borne photographs.

The first useful photographs of the Western Desert of Egypt were obtained by the Gemini missions. These photographs provided views of the remote southwestern regions and allowed mapping of the morphology (Pesce, 1968). One particular photograph with large regional coverage (S-66-54528) vividly portrayed the flow directions of sand dune belts among the topographically-high plateaus and granitic mountains (Fig. 4.3).

A near vertical view of the Uweinat Mountain was also obtained by the Gemini XI mission (S-66-54776). Taken from an altitude of 482 km, the photograph showed the details of the mountains of Uweinat,



Figure 4.3 The eastern Sahara as viewed by Gemini XI, photograph number S-66-54528.

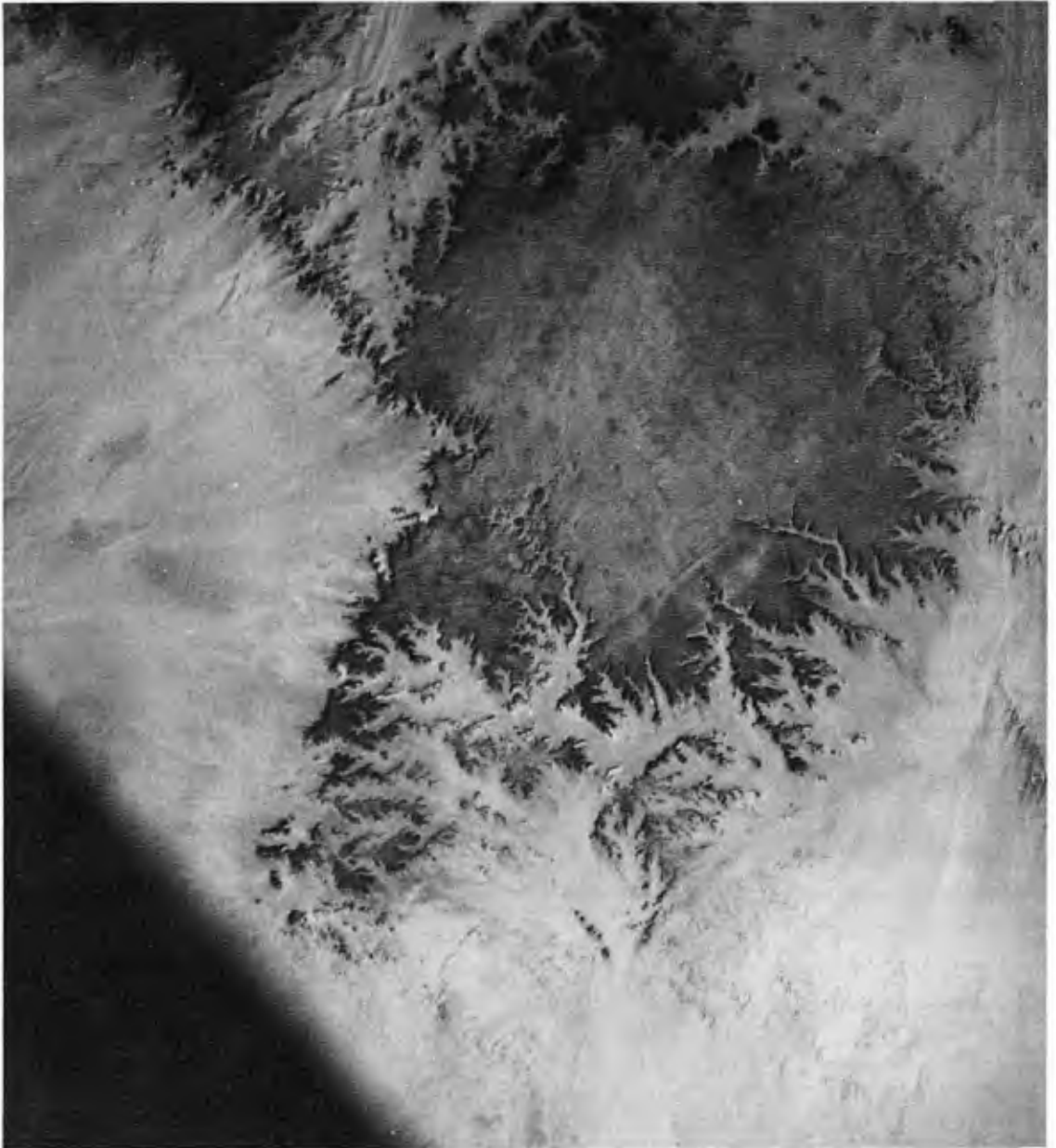


Figure 4.4 Apollo 7 view of the Gilf Kebir plateau. Width of photograph at top is approximately 140 km.

Archenu, Kissu, and Babein, all of which are circular granitic intrusions (Pesce, 1968, p. 62). The same view showed details of the southern Gilf Kebir and the diversity in the directions of dune belts as they made their way between the topographic highs.

Perhaps the best photograph of the Gilf Kebir plateau was obtained by Apollo mission 7 (Fig. 4.4). The southern half of the

Gulf was depicted as a flat and smooth-surfaced plateau with straight western borders. The photograph clearly displayed the numerous deep canyons particularly in the southeastern border. The canyons were clearly formed by water erosion under rainy conditions, which prevailed over 8,000 years ago. These canyons were morphologically compared to similar gorges in the martian canyonlands (Maxwell and El-Baz, 1979).

Apollo mission 9 obtained two noteworthy photographs of the southern part of the Western Desert of Egypt. The first, AS9-23-2533, depicted the Uweinat Mountain region, particularly the sand dune belts in southwest Egypt (Nicks, 1970). The second, AS9-20-3176, showed the vast plains of the southeastern part of the desert. In this photograph east-west trending scarps were clearly displayed along with patches of light-colored deposits, which marked the sites of ancient playa deposits of former lakes.

The Skylab astronauts also obtained useful photographs of the southern part of the Western Desert of Egypt. Two photographs in particular provided new information on the Darb El-Arba'in Desert (as named by Vance Haynes in this volume), in the southeast (SL4-138-3770), and on the extension of features in the southwest part deep into Sudan (SL3-115-1900). In the latter photograph, it is clear that the light-colored streaks in Egypt extend into the Sudan with a distinct veering towards the southwest (Fig. 4.5). The scarps and isolated hills typi-



Figure 4.5 Skylab 3 photograph of the southwestern desert of Egypt and the northwestern desert of Sudan, showing the curved nature of eolian streaks (SL3-115-1900).

cal of the Western Desert are also prevalent in northwestern Sudan. The numerous color variations in this photograph are not yet fully understood.

Photography of the deserts of Egypt was considered a major objective on the Apollo-Soyuz Test Project (ASTP). ASTP photographs were obtained with one Nikon and two Hasselblad 70mm cameras (Table 4.1). One 70mm camera was bracket-mounted and was equipped with an intervalometer and reseau plate to provide stereo mapping photography. The second camera had a single lens reflex mechanism for handheld photography. Some photographs were taken with a color sensitive film (SO-242) that was specifically selected for desert photography (El-Baz, 1977).

The ASTP photographic coverage is shown in Figure 4.6. Some of the photographs covered areas previously photographed on earlier missions, for example the Uweinat Mountain region (Fig. 4.7). This allowed making comparisons of the two data sets to study changes with time. Using a Bausch and Lomb model ZT-4 Zoom Transfer Scope, one photograph can be projected onto another, despite differences in obliquity and scale, by optically rotating, stretching, and enlarging one of the photographs.

One such comparison was made of the Uweinat Mountain region (Slezak and El-Baz, 1979). As shown in Figure 4.7, the wind-deposited

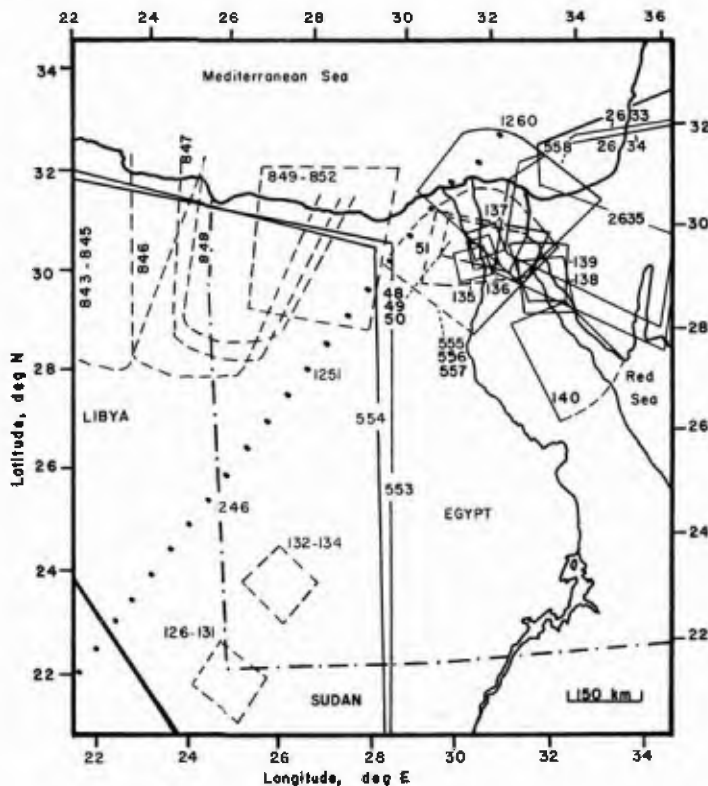


Figure 4.6 Photographic coverage of Egypt from the Apollo-Soyuz Test Project. Numbers are listed in Table 4.1.

sand between the mountain highs is much lighter in color than the surroundings. The region was analyzed in an effort to determine the temporal changes that may have occurred between the time of the Apollo 9 photograph that was taken in 1969 (AS9-23-3533) and the ASTP photographs that were taken in 1975 (AST-2-126, 127, 129, and 130). It was found that the lateral shift distance of sand in the region was 2.5 km in 6 years, or more than 400 m per year (Slezak and El-Baz, 1979, p. 269).

#### LANDSAT IMAGES

The unmanned Landsat satellites operate from the relatively high altitude of approximately 920 km. Landsat spacecraft are in a near-polar orbit (81° inclination) and travel around the Earth every 103 minutes. Therefore, they fly over the same area of the Earth every 18 days. Each spacecraft is equipped with scanners that image portions of the Earth on selected orbit.

The Landsat multispectral scanners produce images representing four different bands of the electromagnetic spectrum. The four black-and-white bands are designated as follows: band 4 for the green spectral region (0.5 to 0.6 microns); band 5 for the red spectral region (0.6 to 0.7 microns); band 6 for the near-infrared region (0.7 to 0.8 microns); and band 7 also for the near-infrared region (0.8 to 1.1 microns).



Figure 4.7 Apollo-Soyuz photograph of the Uweinat Mountain region. Note the bright sand dune belts between the topographic highs (AST-2-127).

Light reflectance data from the four scanner channels are converted first into electrical signals, then into digital form for transmission to receiving stations on Earth. The recorded digital video data are re-formatted into computer compatible tapes and/or converted at special processing laboratories to black-and-white photo images. The images from the four bands can be recorded on four black-and-white films from which photographic prints are made in the usual manner.

Because each of the four bands records a different range of radiation, the black-and-white images generated for each band display different sorts of information. Combinations of three or four of the bands produce false-color composites. Such composites covering the total area of Egypt (Fig. 4.2), have been made, annotated and published (El-Baz, 1979a).

The effective resolution of Landsat images at 1:1,000,000 scale is approximately 400 m. However, the Landsat data can be computer-enhanced to produce images at 1:250,000 scale and larger. The effective resolution of enhanced images becomes about 150 m, which is double the size of individual picture elements (one "pixel" = 80 m). However, linear and very high-contrast features the size of a pixel can be detected in such enhanced images.

The difference between the standard and enhanced Landsat products is shown in Figure 4.8. The standard image shows part of the Nile Valley in the upper right corner and the Kharga Depression in the lower left. Terrain characteristics are barely discernible in this image. Only the bright-colored dune belts within the dark-floored Kharga depression are barely visible. However, the enhanced image of part of the Kharga depression clearly displays the lineated nature of the yardang field north of Kharga. This image also shows the texture of sand dune belts and the road that connects Kharga with Dakhla Oasis to the west and the Nile Valley to the northeast.

To date, only a few images covering the Western Desert oases and the Uweinat Mountain - Gilf Kebir region have been enhanced. The cost of this computer enhancement, over \$1,000 per image, has limited the amount of Landsat images that are fully utilizable in photogeologic interpretations.

Landsat spacecraft 1, 2 and 3 were also equipped with a television camera system referred to by the acronym RBV, for return beam vidicon. This system was shut down early in Landsat 1 operation and only worked occasionally on Landsat 2. Digital images from the RBV contain additional information, in the visible range, to the multispectral data. For this reason it was recently recommended to NASA to acquire RBV images of the Western Desert from Landsat 3.

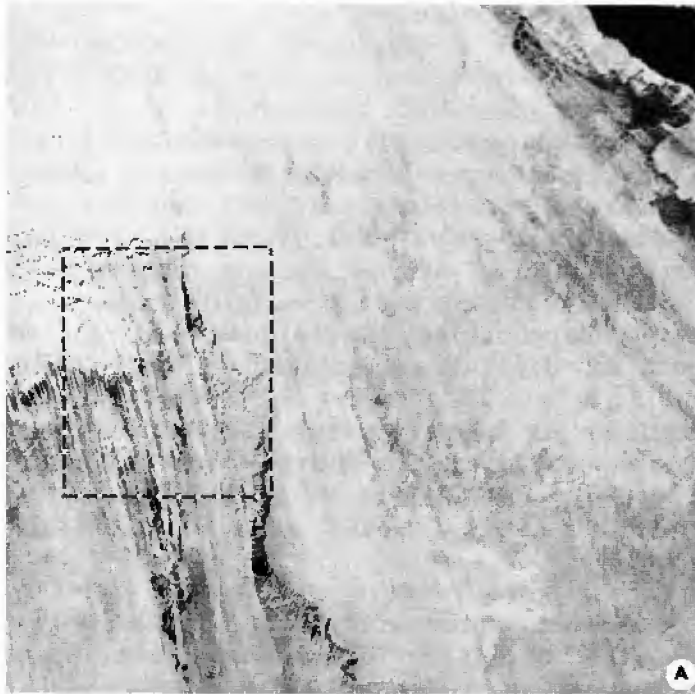


Figure 4.8 (A) Landsat image of the Kharga depression (lower left) and part of the Nile Valley (upper right corner); (B) Computer enhanced part of image marked by a box in (A).

## RECOMMENDATIONS FOR FUTURE MISSIONS

### The Large Format Camera

The Space Shuttle program will allow the application of what has been learned on previous space missions to better photograph the Earth from orbit. The earliest such use will be of the "Large Format Camera" (LFC; as shown in Fig. 4.9) to allow the acquisition of mapping quality, vertical, stereo, color, and high-resolution photographs from orbit. Photographs from this camera can be used for mapping utilizing conventional techniques and instruments without costly electronic and digital enhancement or image correction.

The LFC derives its name from the size of its individual frames; 45.7 cm in length and 22.9 cm in width. Its 305 mm, f/6 lens has a  $40^\circ \times 74^\circ$  field-of-view. The film will be driven by a forward motion compensation unit as it is exposed on a vacuum platen (El-Baz and Ondrejka, 1978).

The LFC system resolution will be 100 lines/mm (1000:1 contrast) to 88 lines/mm (2:1 contrast). This means a photo-optical resolution of 10 to 20 m from an altitude of 260 km. The camera will have the ability to utilize a number of films, including Kodak high resolution black-and-white (3414), color (SO-356), and color infrared (SO-131) in magazines with a capacity of 1,200 m of film. Also an electronic filter changer will permit different films to be used during a single mission.

Orthophotomaps may be made from LFC orbital photographs at scales of 1:100,000 and 1:50,000. The operating framing rate of 80% will provide the required base/height ratio for topographic mapping with 20 m contours (Doyle, 1979).

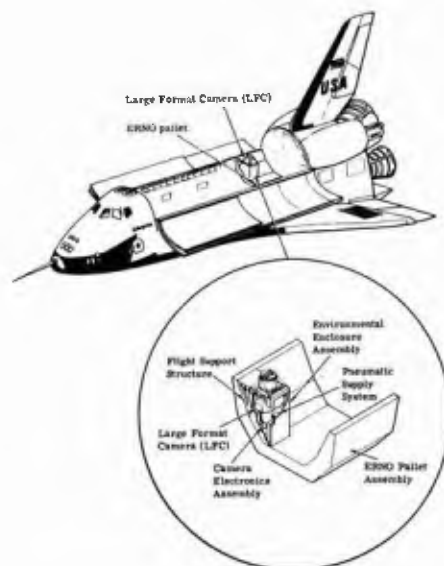


Figure 4.9 Sketch illustrating the deployment of the Large Format Camera (LFC) in the Space Shuttle cargo bay (from El-Baz and Ondrejka, 1978, p. 716).

Both the resolution and the geometric accuracy of the LFC make it very suitable for photography of the southern part of the Western Desert of Egypt. It is recommended that such photographs be taken to allow geologic interpretations and the making of large scale topographic maps. High resolution photographs and accurate topographic maps are required for detailed study of this region, both for its development potential and for analog correlation with the martian deserts.

### The SPOT System

The European Space Agency has adopted the SPOT system as one of its major earth observation programs. SPOT is a multi-mission platform that was initiated as part of the national space program of France (Honvault, 1980), with the first satellite to be launched in 1985 using an Ariane rocket.

The basic data acquisition system is composed of two imaging instruments in the visible and near-infrared spectra within a 60 km field-of-view. These instruments utilize the recently-developed "linear array" detector technology rather than the Landsat type "scanners". The detectors will allow the acquisition of images with the ground resolution of 20 m in the multispectral (3 band) mode, and 10 m in the panchromatic mode.

SPOT instruments will also be able to acquire stereoscopic images of the same area of the Earth. This will be accomplished by a mirror placed in the opening of each instrument that may be swiveled  $\pm 26^\circ$ . This mirror will allow the instruments to acquire images of areas as distant from the satellite groundtrack as 400 km. With the satellite placed in a sun-synchronous  $98.7^\circ$  inclination orbit at 822 km above Earth, it will cover the globe in 26 days, with access to a given area at an average of 2.5 days. The platform mass of SPOT is 920 kg with a maximum payload mass of 800 kg. With the solar power panels extended it will measure 6 m in length by 12 m in width. The spectral bands of each sensor will cover the following ranges: (a) 0.50 - 0.59 microns, 0.61 - 0.69 microns, and 0.79 - 0.90 microns for the three multi-spectral bands (20 m resolution); and (b) 0.50 - 0.90 microns for the panchromatic sensor (10 m resolution).

Both the resolution and the stereo coverage of the panchromatic sensor make it suitable for photography of subtle topographic features, such as those of the Western Desert. SPOT images should be obtained of this desert for use in photogeologic interpretations and for analog correlations with features of Mars.

## REFERENCES

- Cortright, E. M., 1968, Exploring Space with a Camera: NASA SP-168, Wash. D.C., 214 p.
- Doyle, F. J., 1979, A large format camera for shuttle: Photogramm. Eng. and Remote Sens., v. 45, p. 73-78.
- El-Baz, F., 1977, Astronaut Observations from the Apollo-Soyuz Mission: Smithsonian Studies in Air and Space, No. 1, Wash. D. C., Smithsonian Institution Press, 400 p.
- , 1978a, The meaning of desert color in Earth orbital photographs: Photogramm. Eng. and Remote Sens., v. 44, p. 69-75.
- , 1979a, Egypt as seen by Landsat: Cairo, Egypt, Dar Al-Maaref.
- El-Baz, F. and Ondrejka, R. J., 1978, Earth Orbital Photography by the Large Format Camera: Proc. 12th Internat. Symp. on Remote Sensing of Environment, v. 1., Environmental Research Institute of Michigan, Ann Arbor, p. 703-718.
- Honvault, C., 1980, The earth resources satellite programme of the European Space Agency (abstract): in Summaries, 14th International Symposium on Remote Sensing of the Environment: Ann Arbor, Mich., Environmental Research Inst. of Michigan, p. 8.
- Maxwell, T. A. and El-Baz, F., 1979, Fluvial landforms in Southwestern Egypt: Implications for surface processes on Mars (abstract): in Lunar and Planetary Science X, Lunar and Planetary Institute, Houston, Texas, Part 2, p. 786-788.
- Nicks, O. W., 1970, This Island Earth: NASA SP-250, Wash. D. C., 182 p.
- Pesce, A., 1968, Gemini Space Photographs of Libya and Tibesti: A Geological and Geographical Analysis: Petroleum Exploration Society of Libya, Tripoli, Libya, 81 p.
- Said, R., 1962, The Geology of Egypt: Amsterdam, Elsevier Pub. Co., 377 p.
- Slezak, M. H. and El-Baz, F., 1979, Temporal changes as depicted on orbital photographs of arid regions in North Africa: in El-Baz, F. and Warner, D. M., eds., Apollo-Soyuz Test Project Summary Science Report, Volume II: Earth Observations and Photography: NASA SP-412, Wash. D. C., p. 263-272.